

# Modeling of liquid film flow in annuli

Henryk Anglart\*

*Institute of Heat Engineering, Warsaw University of Technology  
21/25 Nowowiejska Street, 00–665 Warsaw, Poland*

## Abstract

One of the challenges in thermal-hydraulic analyses of BWRs is correct prediction of dryout occurrence in fuel assemblies. In practical applications the critical powers in fuel assemblies are found from correlations that are based on experimental data. The drawback of this approach is that correlations are valid only for these fuel assemblies on which the experiments have been conducted. Other restrictive factors are the limited ranges of experimental working conditions including pressure, mass flux and axial power distributions. To overcome the above-mentioned limitations, several different approaches have been proposed to predict the dryout occurrence. One of them is to employ a phenomenological model of annular flow, in which the mass transfer between the liquid film and the gas core is based on entrainment and deposition correlations. Most of these correlations are derived from water-air flows in vertical tubes and their applicability to other geometries in general, and rod-bundles in particular, should be analysed. This paper presents an analysis of the entrainment rate in vertical annuli. Using the standard approach to calculate the entrainment rate, one can demonstrate that the results deviate from measurements. It has been shown that modifying the entrainment correlation based on data obtained in the annulus geometry leads to an essential improvement in the predictive capability of the phenomenological model of annular two-phase flow.

*Keywords:* Entrainment rate, Annular flow, Dryout, Annular geometry, BWR

## 1. Introduction

An accurate prediction of dryout occurrence in fuel assemblies of a Boiling Water Reactors (BWR) is very important for an economical and safe operation of nuclear power plants. Due to complexity of the governing phenomena, the dryout occurrence is still predominantly evaluated by using specific correlations rather than computational models. This is particularly true when performing safety and licensing analyses for nuclear power plants where specific correlations, derived from experimental data

obtained in full-scale dryout test, exhibit higher accuracy than corresponding general-purpose computational models. The drawback of correlations is that they are limited to the test conditions (including both geometry and operational conditions) and their derivation is very expensive. As a result, there is a growing interest to develop accurate, general-purpose computational models for the dryout occurrence.

During the past fifty years, the dryout conditions have been tested by several researches using various types of test sections and applying a wide range of operational conditions. Majority of experiments have been performed in tubes, e.g. Bennet et al. [1],

\*Corresponding author

Email address: [henryk@kth.se](mailto:henryk@kth.se) (Henryk Anglart\*)

Nigmatulin [2], Milashenko et al. [3] and Adamson and Anglart [4]. In this paper a special interest is directed towards experiments performed in annuli, where both the rod and the tube are heated. Such experiments have been performed by, e.g. Becker and Letzter [5], Becker and Letzter [6], Wurtz [7], Behamin et al. [8], Anglart and Persson [9] and Anghel and Anglart [10]. In such experiments it was observed that the dryout occurs exclusively on the rod surface rather than on the tube when equal heat flux is applied for both heated surfaces. Moeck [11], Manov [12] and Wurtz [7] measured film flow rates on both the rod and the tube wall and discovered that the tube film flow per unit perimeter is 2 to 5 times greater than corresponding rod film flow rate. Andersen and Wurtz [13] applied the radiation theory based on the Lambert's Cosine Law to explain the asymmetric distribution of liquid films but concluded that the theory cannot predict the observed distribution. Whalley and Hutchinson [14] indicated that the radiation theory leads inevitably to the conclusion that for fully developed flow entrainment rates on both walls are equal. They pointed out that the entrainment process is explosive and appears to project droplets in all directions. Due to that an asymmetric distribution of liquid films is obtained.

In this paper standard models for annular flows have been applied for various annular channels. It has been observed that the applied models predict approximately the same film flow rate per unit perimeter for both the rod and the tube film. These results are in clear contradiction with the experimental observations and indicate a need for a revision of the correlations for the entrainment and deposition rates in annuli.

## 2. Model of film flow in annular geometry

Current state-of-the-art approach to predict dryout occurrence in a boiling channel is to predict the liquid film flow rate on heated walls. Those locations where the liquid film disappears from heated walls will undergo the boiling transition resulting in dryout. The key issue in this type of approach is to formulate a proper mass balance equation for the liquid film. The most common approach is to take into account three different mechanisms of the mass transfer

from the liquid film: entrainment and deposition of liquid drops as well as evaporation on the surface of the liquid film. The entrainment and deposition rates are predicted from various correlations, whereas the evaporation rate is found from the local heat balance, assuming saturation conditions in the liquid film.

This type of phenomenological approach has been explored by several researches. One of the first such models valid for tubes was developed by Whalley et al. [15]. The model was extended to annuli (Whalley [16]) and rod bundles (Whalley [17]). A significant improvement of the model was proposed by Govan et al. [18] and transient capabilities to the model were introduced by Hewitt and Govan [19]. Nigmatulin et al. [20] used the same approach and validated predictions against various experimental data. Okawa et al. [21] proposed own set of correlations for entrainment and deposition and applied the model to prediction of dryout. The model was validated against a large experimental database and it was concluded that the model agreed fairly well with experimental data.

For steady-state flows in tubes, all above-mentioned models are based on the following basic mass conservation equations:

$$\frac{dW_G}{dz} = P_F \Gamma \quad (1)$$

$$\frac{dW_{LE}}{dz} = P_F (E - D) \quad (2)$$

$$\frac{dW_{LF}}{dz} = P_F (D - E - \Gamma) \quad (3)$$

Here  $W_G$ ,  $W_{LE}$  and  $W_{LF}$  are mass flow rates of vapour, entrained liquid and liquid film, respectively;  $z$  is the axial distance,  $P_F$  is the perimeter of the liquid film,  $D$  is the deposition rate,  $E$  is the entrainment rate and  $\Gamma$  is the evaporation rate. There are several different correlations sets for entrainment and deposition rates, which are available in the open literature. The majority of these correlations are based on experimental data obtained mainly in tubes, with air and water as working fluids.

The model given by Eqs. (1) through (3) can be easily extended to annular flow in annuli, where two liquid films are present. Putting the equations in a

dimensionless form, the phenomenological model of annular flow in annuli is as follows,

$$\frac{dx_G}{d\zeta} = Bo_{LFr} + Bo_{LFt} \quad (4)$$

$$\frac{dx_{LE}}{d\zeta} = e_{LFr} + e_{LFt} - (d_{LFr} + d_{LFt}) \quad (5)$$

$$\frac{dx_{LFr}}{d\zeta} = d_{LFr} - e_{LFr} - Bo_{LFr} \quad (6)$$

$$\frac{dx_{LFt}}{d\zeta} = d_{LFt} - e_{LFt} - Bo_{LFt} \quad (7)$$

where  $\zeta = z/d_h$  is the dimensionless axial distance,  $d_h$  is the hydraulic diameter,  $x_j = W_j/W_T$  is the mass fraction of component  $j$ , ( $j = G$  for vapor,  $j = LE$  for entrained liquid,  $j = L_{Fr}$  for liquid film on rod,  $j = L_{Ft}$  for liquid film on tube),  $W_T$  is the total mass flow rate,  $Bo_j = P_{Fj}d_h q_j'' / (W_T h_{fg})$  is the boiling number for liquid film  $j$ ,  $e_j = P_{Fj}d_h E_j / W_T$  is the dimensionless entrainment rate for film  $j$  and  $d_j = P_{Fj}d_h D_j / W_T$  is the dimensionless deposition rate for film  $j$ .

### 3. Evaluation of entrainment and deposition correlations

The deposition rate proposed by Govan et al. [18] is as follows,

$$D = kC \quad (8)$$

where the deposition coefficient  $k$  is found as,

$$k = \begin{cases} \frac{0.18}{\sqrt{\frac{\rho_G d_h}{\sigma}}} & \text{if } \frac{C}{\rho_G} \leq 0.3 \\ \frac{0.083}{\sqrt{\frac{\rho_G d_h}{\sigma}}} \left(\frac{C}{\rho_G}\right)^{-0.65} & \text{if } \frac{C}{\rho_G} > 0.3 \end{cases} \quad (9)$$

where  $\rho_G$  is the density of the gas phase,  $\rho_L$  is the density of the liquid phase,  $\sigma$  is the surface tension and the drop concentration  $C$  in the gas core is given as,

$$C = \frac{G_{LE}}{\frac{G_{LE}}{\rho_L} + \frac{G_G}{\rho_G}} \quad (10)$$

Here  $G_{LE}$  and  $G_G$  are the mass flow rates of the entrained liquid and the gas phase, respectively. The entrainment rate correlation proposed by Govan et al. [18] is as follows,

$$E = 5.75 \cdot 10^{-5} \left[ (G_{LF} - G_{LFC})^2 \frac{d_h \rho_L}{\sigma \rho_G^2} \right]^{0.316} G_G \quad (11)$$

where  $G_{LFC}$  is the critical film mass flux for the onset of entrainment, given as,

$$G_{LFC} = \exp\left(5.8504 + 0.4249 \frac{\mu_G}{\mu_L} \sqrt{\frac{\rho_L}{\rho_G}}\right) \frac{\mu_L}{d_h} \quad (12)$$

where  $\mu_G$  and  $\mu_L$  are the dynamic viscosities of the gas and the liquid phase, respectively.

Bertodano et al. [22] proposed the entrainment rate correlation as follows,

$$\frac{Ed_H}{\mu_L} = 4.47 \times 10^{-7} \left[ We_G \left( \frac{\rho_L - \rho_G}{\rho_G} \right)^{1/2} (Re_{LF} - Re_{LFC}) \right]^{0.925} \left( \frac{\mu_G}{\mu_L} \right)^{0.26} \quad (13)$$

where the following new quantities are introduced:

$$We_G = \frac{\rho_G j_G^2 d_h}{\sigma} \quad (14)$$

$$Re_{LF} = \frac{\rho_L j_{LF} d_h}{\mu_L} \quad (15)$$

$$Re_{LFC} = 80 \quad (16)$$

Here  $j_G$ ,  $j_{LF}$  are the superficial velocities of the gas phase and the liquid film, respectively.

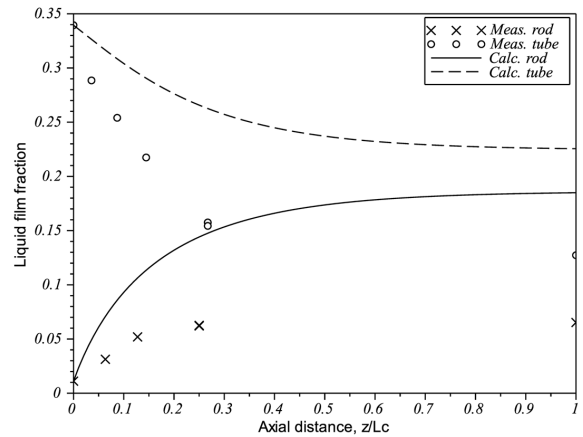


Figure 1: Measured and calculated liquid film flow rates on rod and tube walls in  $5000 \times 23.77 \times 19.71$  mm annulus, using the Govan et al. entrainment correlation. Total mass flux  $1360 \text{ kg/m}^2\text{s}$ , inlet quality 0.38, system pressure 6.89 MPa

The model of liquid film flow in annuli given by Eqs. (4) through (7) has been applied to predict the developing annular flow in  $5000 \times 23.77 \times 19.71$  mm

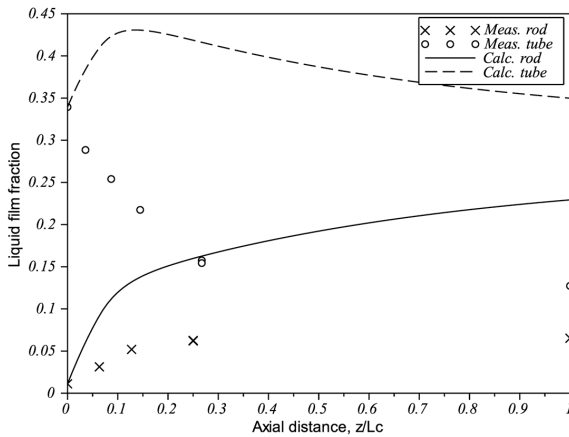


Figure 2: Measured and calculated liquid film flow rates on rod and tube walls in  $5000 \times 23.77 \times 19.71$  mm annulus, using the Bertodano et al. entrainment correlation. Total mass flux  $1360 \text{ kg/m}^2\text{s}$ , inlet quality 0.38, system pressure 6.89 MPa

annulus. The results of calculations are compared with experimental data obtained by Moeck [11]. Since flow is adiabatic, only entrainment and deposition of drops are responsible for the change of mass flow rate of liquid films on the rod and the tube walls. The deposition rate has been calculated from the correlation given by Govan et al. [18], presented in Eqs. (8) through (12). For the entrainment rate calculation both the Govan et al. correlation (Eqs. 11 and 12) and the Bertodano et al. correlation (Eqs. 13 through 16) are used. The comparisons of predictions with Moeck's data are shown in Figs. 1 and 2.

As can be seen, in both cases the predicted flow rates for the liquid film are much higher than measured ones. The experimental data indicate that the flow rate of the liquid film on the tube wall is decreasing, whereas the flow rate of the liquid film on the rod wall is increasing. After approximately  $2/3$  of the pipe length the film flow rates are in equilibrium and fully-developed flow conditions are established. The Govan et al. correlations give a similar asymptotic behaviour; however, the equilibrium flow rates are higher than the measured ones. The Bertodano correlation in Fig. 2 gives an initial increase of the film flow rate, which doesn't agree with the measured data. In addition, as for the Govan correlation, the exit (asymptotic) film flow rates are significantly higher than the measured ones.

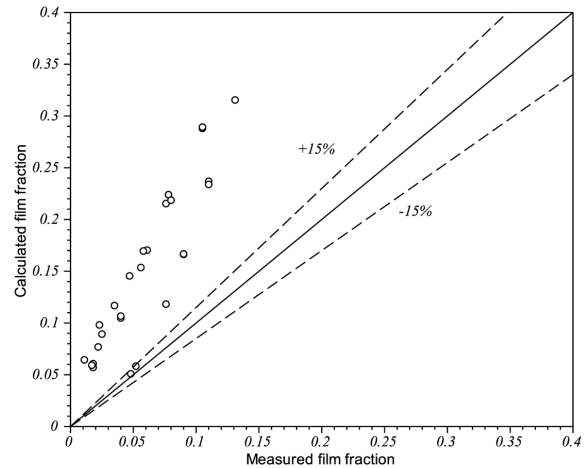


Figure 3: Measured (Mannov) and calculated (Eqs. 4–12) exit liquid film flow rates on rod wall in  $3500 \times 27.2 \times 17$  mm adiabatic annulus. Total mass flux  $400\text{--}2000 \text{ kg/m}^2\text{s}$ , system pressure 7 MPa

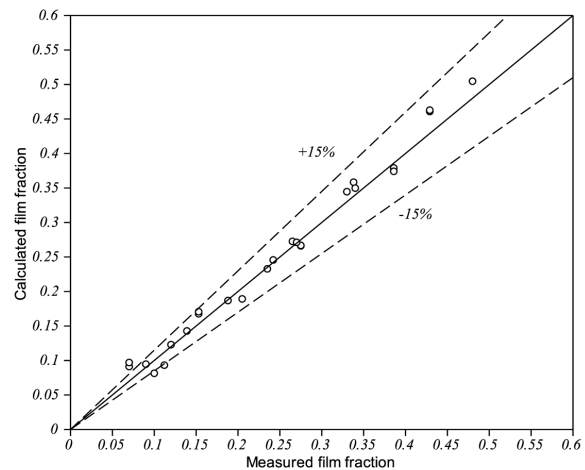


Figure 4: Measured (Mannov) and calculated (Eqs. 4–12) exit liquid film flow rates on tube wall in  $3500 \times 27.2 \times 17$  mm adiabatic annulus. Total mass flux  $400\text{--}2000 \text{ kg/m}^2\text{s}$ , system pressure 7 MPa

Comparisons of the Govan correlations with the experimental data obtained in  $3500 \times 27.2 \times 17$  mm annulus by Mannov [12] are shown in Figs. 3 through 6. Figure 3 shows the measured and calculated exit film flow fraction on the rod surface in adiabatic annulus. Consistently with results shown in Fig. 1, the calculated exit film flow rates are significantly higher than the calculated ones. Interestingly, the calcu-

lated exit film flow fraction on the tube wall, shown in Fig. 4, is in good agreement with measured values. However, this is only coincidental, since the entrained rate in the annulus is underestimated, which causes in turn underestimation of the deposition rate on both the rod and the tube surface.

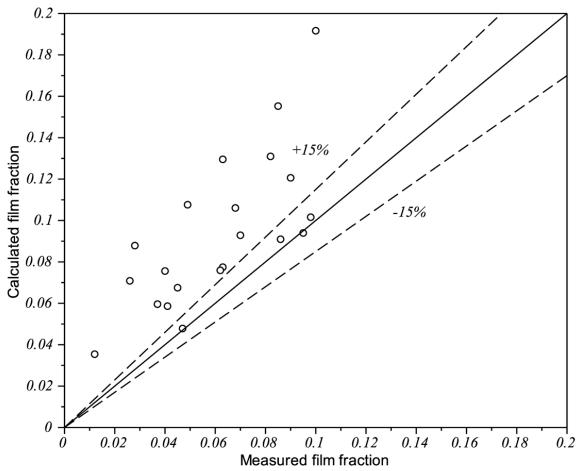


Figure 5: Measured (Mannov) and calculated (Eqs. 4÷12) exit liquid film flow rates on rod wall in  $3500 \times 27.2 \times 17$  mm with heated rod. Total mass flux  $400\text{--}2000$  kg/m<sup>2</sup>s, system pressure 7 MPa

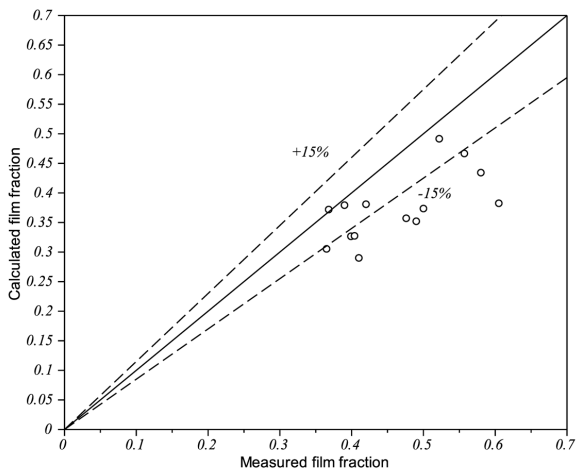


Figure 6: Measured (Mannov) and calculated (Eqs. 4÷12) exit liquid film flow rates on tube wall in  $3500 \times 27.2 \times 17$  mm with heated rod. Total mass flux  $400\text{--}2000$  kg/m<sup>2</sup>s, system pressure 7 MPa

For cases with a heated rod, the comparisons of cal-

culations with measured data are shown in Figs. 5 and 6. The results exhibit somewhat increased scatter, which probably results from evaporation effects on the liquid film.

Results presented in Figs. 1 through 6 demonstrate a significant discrepancy between predicted and measured film flow rates on the rod surface. For liquid film on the tube surface the predicted results are generally in better agreement with measurements (clearly visible in Fig. 4), even though some discrepancies are present (as seen in Fig. 1). This dissimilar behaviour of liquid films on the rod and the tube surfaces suggests that the deposition and entrainment rates may be different for the two surfaces.

#### 4. Modified entrainment correlations

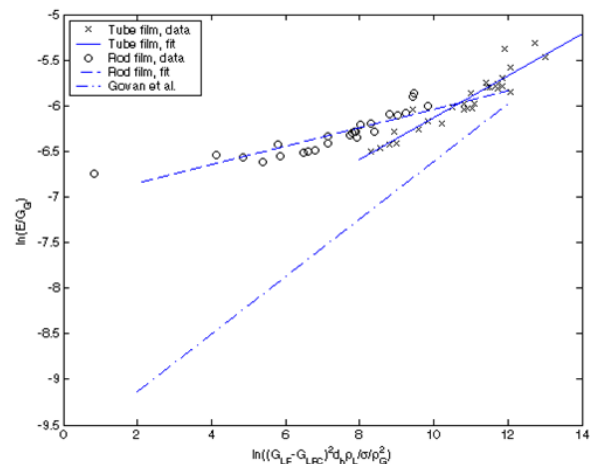


Figure 7: Entrainment rate in annulus estimated from Moeck data and using the Govan et al. correlation for the deposition rate

The Moeck data for developing liquid films in an annulus can be used to derive the entrainment rate as a function of local liquid film mass flux. Assuming that the deposition rate is the same for the rod and the tube film, the derived entrainment rates are as shown in Fig. 7. As can be seen the derived entrainment rate on the rod surface is much higher than the entrainment rate obtained from the Govan correlation. This is particularly true for low values of the following non-dimensional parameter,

$$\Omega = \ln \left[ \frac{(G_{LF} - G_{LFC})^2 d_h \rho_L}{(\sigma \rho_G^2)} \right] \quad (17)$$

which is used as an independent variable in Fig. 7.

The results shown in Fig. 7 indicate that assuming the same deposition rates on both the rod and the tube walls, the entrainment rates are different for the two surfaces. Even though this result is quite convincing, it has been obtained for an annulus with a rather small hydraulic diameter ( $d_h = 4$  mm) and thus must be treated with caution when applied to other annuli and geometries.

Similar analysis can be performed for fully-developed adiabatic annular flow data. In this case, Eqs. (4) through (7) become,

$$\frac{dx_G}{dS} = 0 \quad (18)$$

$$0 = e_{LFr} + e_{LFt} - (d_{LFr} + d_{LFt}) \quad (19)$$

$$0 = d_{LFr} - e_{LFr} \quad (20)$$

$$0 = d_{LFt} - e_{LFt} \quad (21)$$

Eq. (19) can be dropped since it results from Eqs. (20) and (21). It is clear that Eqs. (20) and (21) are not satisfied when applying any correlations considered in this paper and using experimental data obtained in annuli. In other words, using mass flow fractions of liquid films, vapour and the entrained liquid and substituting to the deposition and entrainment correlations it can be seen that

$$d_{LFr} - e_{LFr} = \varepsilon_r \neq 0 \quad (22)$$

$$d_{LFt} - e_{LFt} = \varepsilon_t \neq 0 \quad (23)$$

Assuming further that the modified correlation for the entrainment rate has the same form as given in Eq. (11), that is:

$$E = a \left[ (G_{LF} - G_{LFC})^2 \frac{d_h \rho_L}{\sigma \rho_G^2} \right]^b G_G \quad (24)$$

coefficients  $a$  and  $b$  can be derived from a proper experimental data sets. Using data obtained by Andersen and Wurtz [13] for adiabatic steam-water annular flow in annular geometry, the coefficients for the entrainment rate from the rod surface can be obtained as:  $a = 3.323 \cdot 10^{-5}$  and  $b = 0.5$ .

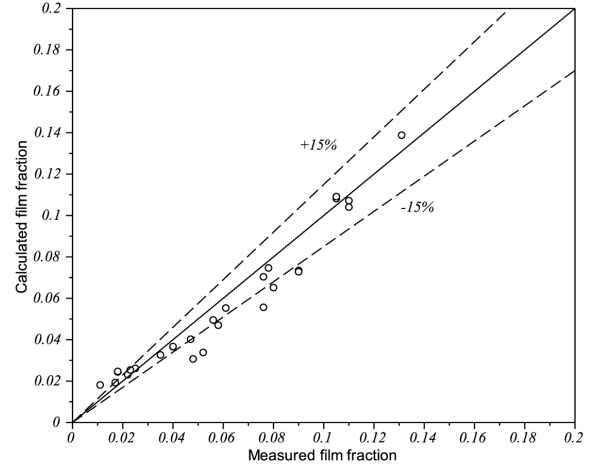


Figure 8: Measured (Mannov) and calculated (Eqs. 4÷12) exit liquid film flow rates on rod wall in  $3500 \times 27.2 \times 17$  mm adiabatic annulus, using modified entrainment rate correlation. Total mass flux  $400\text{--}2000$   $\text{kg/m}^2\text{s}$ , system pressure 7 MPa

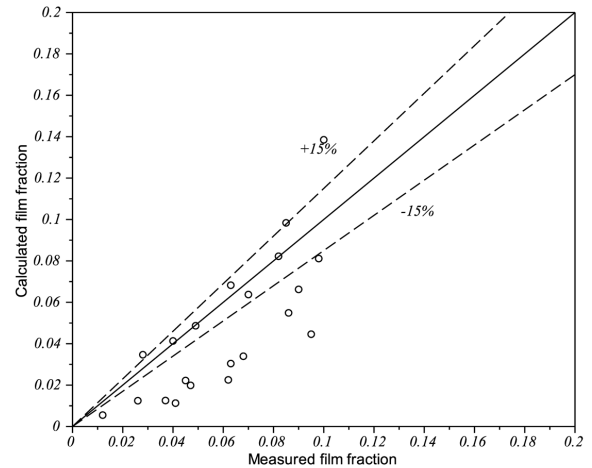


Figure 9: Measured (Mannov) and calculated (Eqs. 4÷12) exit liquid film flow rates on rod wall in  $3500 \times 27.2 \times 17$  mm annulus with heated rod, using modified entrainment rate correlation. Total mass flux  $400\text{--}2000$   $\text{kg/m}^2\text{s}$ , system pressure 7 MPa

Figures 8 and 9 show the predicted film flow rates obtained with the new entrainment correlation for the rod surface, while keeping the standard Govan et al. correlation for the tube surface.

Comparing Fig. 8 with Fig. 3, a significant improvement of prediction accuracy can be seen for adiabatic annulus. Also some improvements of accuracy can be seen for the annulus with heated rod, as can be

deduced from a comparison of Figs. 9 and 5. Somewhat higher scatter in Fig. 9 probably results from the influence of film evaporation on deposition and entrainment rates. Clearly, this effect requires further investigation in order to improve the present model.

## 5. Conclusions

It has been shown that currently available entrainment and deposition correlations are not applicable to an annular geometry. In particular, the liquid film thickness on the rod wall in an annulus is significantly over-predicted using correlations, which have been applied in this paper. It has been shown that modifying the entrainment correlation based on data obtained in the annulus geometry leads to an essential improvement in the predictive capability. However, more work is needed to satisfactorily explain the observed difference in the entrainment rates on surface with various curvatures. Such improvement is particularly needed for application of correlations to predict the dryout occurrence in fuel assemblies of Boiling Water Reactors.

## Acknowledgments

The publication was created in the framework of a strategic project of the Polish National Centre for Research and Development (NCBR): "Technologies for the development of safe nuclear energy", Research Task No. 9 entitled "Development and implementation of safety analysis methods in nuclear reactors during disturbances in heat removal and severe accident conditions".

## References

- [1] A. W. Bennett, G. F. Hewitt, H. A. Kearsy, R. K. F. Keays, D. J. Pulling, Studies of Burnout in Boiling Heat Transfer to Water in Round Tubes with Non-Uniform Heating, AERE-R5076, 1966.
- [2] B. I. Nigmatulin, Investigation of two-phase annular dispersed flows in heated tubes, Appl. Mech. Tech. Phys. 4 (1973) 78–88.
- [3] V. I. Milashenko, B. I. Nigmatulin, V. V. Petukhov, N. I. Trubkin, Burnout and distribution of liquid in evaporative channels of various lengths, Int. J. Multiphase Flow 15 (3) (1989) 393–401.
- [4] C. Adamsson, H. Anglart, Film flow measurements for high-pressure diabatic annular flow in tubes with various axial power distributions, Nucl. Eng. Des. 236 (2006) 2485–2493.
- [5] K. Becker, A. Letzter, An Experimental Study of the Effect of the Axial Flux Distribution on the Burnout Conditions in a 3650 mm Long Annulus, KTH-NEL-21, Stockholm, Sweden, 1974.
- [6] K. Becker, A. Letzter, Burnout Measurements for Flow of Water in an Annulus with Two-Sided Heating, KTH-NEL-23, Stockholm, Sweden, 1976.
- [7] J. Würtz, An experimental and theoretical investigation of annular steam-water flow in tubes and annuli, Risø Report 372, Risø National Laboratory, Denmark (1978).
- [8] D. Behamin, P. Persson, S. Hedberg, J. Blomstrand, Loop studies simulating – in annular geometry – the influence of the axial power distribution and the number of spacers in 8x8 bwr assemblies, in: Proc. Two-Phase Flow Group Meeting, Karlsruhe, Germany, 1999.
- [9] H. Anglart, P. Persson, Experimental investigation of post-dryout heat transfer in annulus with spacers, Int. J. Multiphase Flow 33 (2007) 809–821.
- [10] I. G. Anghel, H. Anglart, Post-dryout heat transfer to high-pressure water flowing upward in vertical channels with various flow obstacles, Int. J. Heat Mass Trans. 55 (2012) 8020–8031.
- [11] E. O. Moeck, Annular-Dispersed Two-Phase Flow and Critical Heat Flux, AECL-3656, 1970.
- [12] G. Mannov, Film flow measurements in concentric annulus 3500x27.2x17 mm with heated and unheated rod, Tech. Rep. SDS-65, Danish Atomic Energy Commission, Riso, Denmark (1973).
- [13] P. S. Andersen, J. Würtz, Adiabatic steam-water annular flow in an annular geometry, Int. J. Multiphase Flow 7 (1981) 235–239.
- [14] P. B. Whalley, P. Hutchinson, Comments on "adiabatic steam-water annular flow in an annular geometry" by p.s. andersen and j. wurtz, Int. J. Multiphase Flow 7 (1981) 241–243.
- [15] P. B. Whalley, P. Hutchinson, G. F. Hewitt, The calculation of dryout in forced convection boiling, in: Fifth International Heat Transfer Conference, Tokyo, Japan, 1974.
- [16] P. B. Whalley, P. Hutchinson, G. F. Hewitt, Prediction of annular flow parameters for transient conditions and for complex geometries, in: European Two-Phase Flow Group Meeting, Haifa, Israel, 1975.
- [17] P. B. Whalley, The Calculation of Dryout in a Rod Bundle, AERE-R 8319, Harwell, U.K., 1976.
- [18] A. H. Govan, G. F. Hewitt, D. G. Owen, T. R. Bott, An improved chf modelling code, in: 2<sup>nd</sup> UK National Heat Transfer Conference, Glasgow, UK, 1988.
- [19] G. F. Hewitt, A. H. Govan, Phenomenological modelling of non-equilibrium flow with phase change, Int. J. Heat Mass Transfer 33 (2) (1990) 229–242.
- [20] R. I. Nigmatulin, B. I. Nigmatulin, Y. D. Khodzhaev, V. E. Kroshilin, Entrainment and deposition rates in a dispersed-film flow, Int. J. Multiphase Flow 22 (1) (1996) 19–30.
- [21] T. Okawa, A. Kotani, I. Kataoka, M. Naito, Prediction of critical heat flux in annular flow using a film flow model,

- J. Nucl. Sci. Techn. 40 (6) (2003) 388–396.
- [22] M. A. Lopez de Bertodano, A. Assad, Entrainment rate of droplets in the ripple-annular regime for small vertical ducts, Nucl. Sci. Eng. 129 (1) (1998) 72–80.
- [23] I. Kataoka, M. Ishii, Mechanism and correlation of droplet entrainment and deposition in annular two-phase flow, Tech. Rep. NUREG/CR-2885, ANL-82-44, Argonne National Laboratory (1982).
- [24] S. Sugawara, Y. Miyamoto, Fidas: Detailed subchannel analysis code based on the three-fluid and three-field model, Nucl. Eng. Des. 120 (1990) 147–161.